論文 Bond Strength of Reinforced Concrete Members Confined with FRP Sheets

Yulia Hayati[*1], Tetsuzo KAKU[*2], Kazunari MATSUNO[*3] and Akiteru OKAMURA[*4]

ABSTRACT: Twenty cantilever type specimens were tested with and without fiber reinforced polymer (FRP) sheet confinement in order to investigate the increase of the bond strength of longitudinal bars in the RC members by the sheet confinement. Test variables were the type of FRP sheet (carbon, aramid and glass), the amount of FRP sheet (0, 0.08, 0.16 and 0.25%). Test result showed that the confinement enhanced the bond strength and ductility, and the bond strength increase due to the FRP sheet was well evaluated by the equation proposed previously by the authors.

KEYWORDS: FRP sheet, carbon, aramid, glass, bond splitting failure, bond strength, cantilever type bond test.

1. INTRODUCTION

It is well known that the confinement by FRP sheets greatly increases the shear capacity of reinforced concrete beams and column. The increase in shear capacity by FRP sheets has been experimentally evaluated and incorporated in design equations[1]. According to a truss analogy, the increase in shear capacity should be guaranteed by also increase of bond stress. However, the increase in bond strength for RC members confined with FRP sheet has not been fully quantified.

From 1998 to 1999, forty cantilever type specimens were tested in Toyohashi University of Technology to study the increase in bond strength for RC members confined with FRP sheets[2]. It was observed there that bond strength increased linealy with elastic modulus and the effectiveness of FRP sheets on the bond strength did not stay constant but decrease as the amount sheets increased. Based on the observation, a design equation was proposed to predict the increase in bond strength due to FRP sheets[3].

In this study, number of longitudinal tested bars was limited to 'three', because the cases of 'two' and 'four' were investigated fully in previous tests[2,3], and the new material, namely, glass fiber reinforced polymer sheet was used in addition with carbon and or aramid. The test results showed that the design equation also can predicted the increase in bond strength in the case of three longitudinal bars and glass fiber sheet.

*1 Dept. of Architecture and Civil Eng, Toyohashi University of Technology, BE, Member of JCI
*2 Dept. of Architecture and Civil Eng, Toyohashi University of Technology, Dr, Member of JCI
*3 Dept. of Architecture, Kure Technical College, Member of JCI
*4 Dept. of Architecture and Civil Eng, Toyohashi University of Technology, BE

2. EXPERIMENTAL PROGRAM

2.1 TEST SPECIMENS

Shown in Fig.1(a) is the cantilever type specimen used in this study. The solid line is considered to be a half of a fictitious simply supported beam shown in a break line. The term 'cantilever' came from the fact that the half of the simply support beam is equivalent to a cantilever beam. The upper three bars were directly pulled as tension reinforcement of a fictitious beam. The bond length was 300 mm and the right 100 mm end was encased with a steel pipe to prevent bond with the surrounding concrete. Two closed stirrup (p_{wf} = 0.186%) were placed around the longitudinal bars as shear reinforcement as shown in Fig.1(a). These longitudinal and shear bars formed the main reinforcement. Supplemental reinforcement made from D10 and D19 was placed inside the main reinforcement to avoid a shear failure. Without FRP confinement the specimen was designed to fail in the side splitting mode according to the design equation of Morita and Fujii[4]. Sheet arrangement is shown in Fig.1(c). One layer of FRP sheet in this configuration corresponds to p_{wf} of 0.08%. For other larger amount p_{wf}, multiple layers of sheets were used.

The mechanical properties of the concrete and reinforcement are shown in Table1 and 2, and those of FRP sheets are shown in Table3. The mix proportions of concrete by weight was 0.63:1.00:3.06:3:55 (water:cement:fine aggregate:coarse aggregate). The maximum aggregate size was 20mm. The details of twenty specimens were summarized in Table 4. Test variables were the type of FRP sheet (carbon, aramid and glass),the amount of FRP sheet(0,0.08,0.16 and 0.25%)and location of tested bar at concrete casting (top or bottom bar), although the diameter (D19) and numbers (3) of the tested bars, the amount of transverse reinforcement (2-φ6@150) and concrete compressive strength (σ_B=31.1N/mm^2) were kept constant.

Table 1: Mechanical properties of concrete

f'_c(N/mm^2)	f_t(N/mm^2)	E_c(N/mm^2)
31.10	2.50	2.43 x 10^4

Table 2: Mechanical properties of steel bar

	f_y (N/mm^2)	f_u (N/mm^2)	E_s (N/mm^2)
D19	720	840	2.00 x 10^5
D10	368	525	1.79 x 10^5
Φ6	277	414	1.80 x 10^5

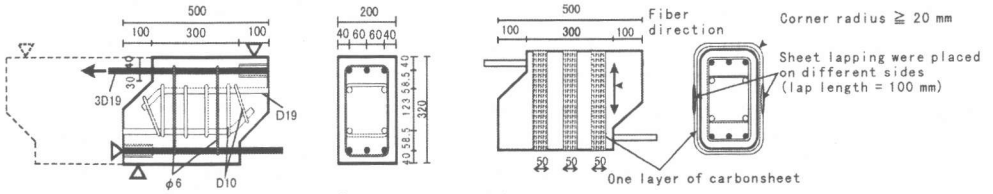

(a) Elevation (b) Section (c) Sheet arrangement for p_{wf}=0.08% of carbon

Figure 1: Specimen details

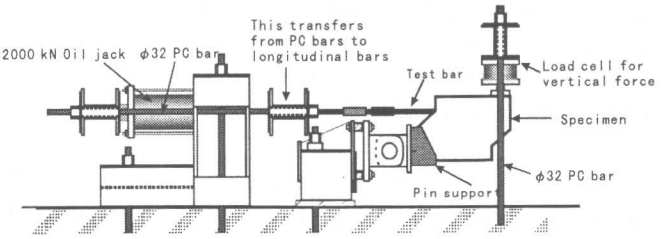

Figure 2: Loading system

2.2 TEST SETUP AND PROCEDURES

The loading system for cantilever specimens is shown in Fig.2. Strains in the FRP sheets at the tested bar level were measured on one side of the specimens. Strains in each tested bar were also measured. After testing of upper bar was completed, the lower bar was tested by rotating the specimen by 180 degree. As the strains on the lower FRP sheet surface were less than 0.02% while the upper bars were tested, the confinement effectiveness by sheets was assumed to be identical for the upper and lower bars.

3. TEST RESULTS AND DISCUSSION

3.1 FAILURE MODES

Almost all specimens failed in side splitting as expected with a little exception as shown in Table 5. Figure 3 shows representative crack patterns of only upper half of the specimen (top bar). Comparing the confined specimens ($p_{wf} = 0.08\%$) with

Table 3: Mechanical properties of FRP sheet

	Carbon	Aramid	Glass
Weight per unit area (gr/m^2)	300	415	900
Specific gravity	1.80	1.45	2.54
Design thickness (mm)	0.167	0.286	0.339
Nominal tensile Strength (N/mm^2)	3400	2000	1370
Nominal elastic modulus (N/mm^2)	$2.30x10^5$	$1.18x10^5$	$0.833x10^5$
Tensile strain of fracture (%)	1.5	1.8	2.0

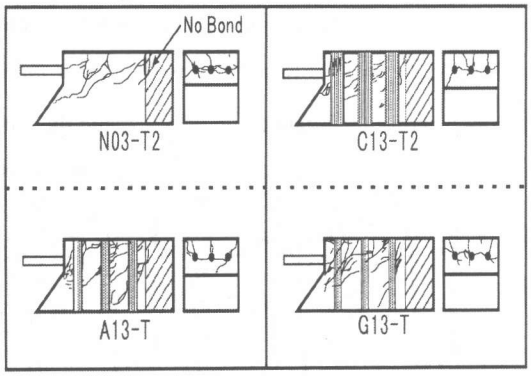

Figure 3: Crack patterns and failure modes

Table 4: Test variable for specimens

Specimen		Variables						
No	Designation	Longitudinal bar			Transverse Reinforcement	FRP sheet		Concrete
		Location of casting *1	Diameter mm	Number of bar		Type of sheet *2	Sheet ratio p_{wf} (%)	σ_b (N/mm^2)
41	N03-T1	T	19	3	2-Φ6 @150 p_{wf} = 0.186%	-	-	31.1
42	N03-B1	B						
43	N03-T2	T						
44	N03-B2	B						
45	C13-T1	T				C	0.08	
46	C13-B1	B						
47	C13-T2	T						
48	C13-B2	B						
49	C23-T	T					0.16	
50	C23-B	B						
51	C33-T	T					0.25	
52	C33-B	B						
53	A13-T	T			*	A	0.08	
54	A13-B	B						
55	A23-T	T					0.16	
56	A23-B	B						
57	G13-T	T				G	0.08	
58	G13-B	B						
59	G23-T	T					0.16	
60	G23-B	B						

*1 T and B represent top and bottom, respectively
*2 C: Carbon A: Aramid G: Glass

no confined that, the number of cracks increased over the wide range of side surface and each crack width became smaller. It was difficult to distinguish the difference of crack patterns of each type of FRP sheet.

3.2 BOND STRESS-SLIP RELATION

Defining the bond stress as the tensile force of tested bar divided by bond length and bar perimeter, the relationship of bond stress and slip at loaded end are shown in Fig. 4. It can be seen regardless of the type of sheet that the bond strength increased and the slope of falling branch after peak load became more gentle as p_{wf} increased.

3.3 INCREASE IN BOND STRENGTH DUE TO FRP SHEET CONFINEMENT

Equation 1 defines the increase of bond strength, $\Delta\tau_{u.}$exp due to confinement

$$\Delta\tau_{u.\exp} = \tau_{u.\exp}(confined) - \tau_{u.\exp}(noconfined) \tag{1}$$

Figure 5 shows the relationship of $\Delta\tau_{u.exp}$ and the number of longitudinal tested bar. The test data at 3

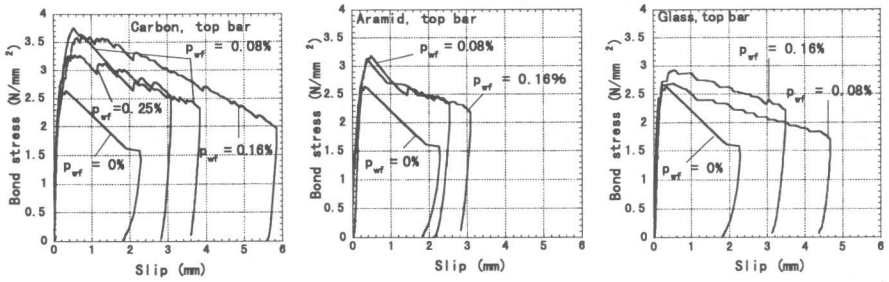

Figure 4 : Bond stress – slip relationship

Table 5: Test Result

No	Designation	Bond strength (exp) $\tau_{u.exp}$ (N/mm^2)	Non dimensioned bond strength (exp.) $\gamma_{u.exp}$	Non dimensioned bond strength (cal.) $\gamma_{u.cal}$	Mode of failure *1
41	N03-T1	2.43	0.53	0.52	Sh
42	N03-B1	3.10	0.56		Sh
43	N03-T2	2.64	0.58		S
44	N03-B2	3.60	0.64		S
45	C13-T1	-	-	0.62	-
46	C13-B1	4.03	0.72		S
47	C13-T2	3.76	0.82		S
48	C13-B2	4.40	0.79		S
49	C23-T	3.61	0.79	0.70	CS
50	C23-B	4.57	0.82		S
51	C33-T	3.28	0.72	0.76	S
52	C33-B	4.71	0.84		S
53	A13-T	3.19	0.70	0.59	S
54	A13-B	4.10	0.74		S
55	A23-T	3.14	0.69	0.64	S
56	A23-B	4.10	0.74		S
57	G13-T	2.70	0.59	0.58	S
58	G13-B	4.02	0.72		S
59	G23-T	2.94	0.64	0.62	S
60	G23-B	4.33	0.78		S

*1 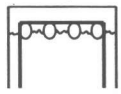 S: Side split failure, 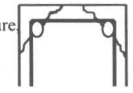 C: Corner split failure, CS: Combine of Corner and Side split failure, Sh: Shear failure

pieces were get from this study and those at 2 and 4 pieces were get from previous paper [2], and the data of which condition is quite same was connected to each other. It can be seen that connected line is not straight but have peak value at 3 pieces. Figure 6 shows the relationship between $\Delta\tau_{u.exp}$ and elastic modulus of used sheet. Although there is one point exception, it can be seen that $\Delta\tau_{u.exp}$ increase with proportional to the elastic modulus of used sheet.

3.4 COMPARIZON THE TEST RESULTS WITH THE DESIGN EQUATION

The experimental value of bond strength in this study was compared with the calculated value by the design equation proposed in previous author's paper[3]. The experimental values were converted to the bond strength of the bottom bar. The design equation (Eq.(2)) is the superposition of Fujii-Morita's equation(Eq.(3) ～ (5)) [4] and experimental equation (Eq.(6)) proposed by author's[3].

$$\tau_{u.cal} = \tau_{cal}^{FM} + \tau_{wf} \quad (2)$$

$$\tau_{cal}^{FM} = \tau_{co.cal} + \tau_{st.cal} \quad (3)$$

$$\tau_{co.cal} / \sqrt{\sigma_b} = 0.117 \cdot b_i + 0.163 \quad (4)$$

$$\tau_{st.cal} / \sqrt{\sigma_b} = 9.51 \cdot p_{ws} \cdot b / (N \cdot d_b) \quad (5)$$

where, $b_i = b_{si} = b/(N \cdot d_b) - 1.0$, σ_b : concrete compressive strength (N/mm^2) N : Number of longitudinal bars, d_b : Diameter of longitudinal bar (mm) , p_{ws} : Transverse reinforcing ratio, b : width of member (mm)

$$\tau_{wf} = \frac{1}{60} \cdot \left(\frac{0.9 \cdot E_{wf}}{E_s} + 0.5 \right) \left(\frac{b}{d_b} \right) \left\{ 1 - \left(\frac{p_{wf}}{0.0035} - 1 \right)^2 \right\} \cdot \sqrt{\sigma_b} \quad (6)$$

where, E_{wf}: elastic modulus of used sheet, E_s: elastic modulus of steel. The comparison is shown in Fig. 7 where the non-dimensioned expression ($\gamma = \tau/\sqrt{\sigma_B}$) was used in order to correspond the arbitrary concrete strength. The previous tested data were also plotted in it. It can be seen that design equation predict the bond strength very well and rather in safety side.

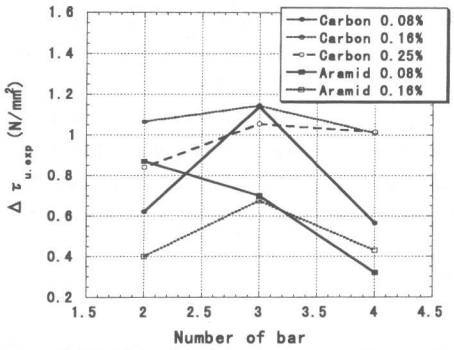

Figure 5: $\Delta\tau_{u.exp}$ – number of longitudinal bar relationship

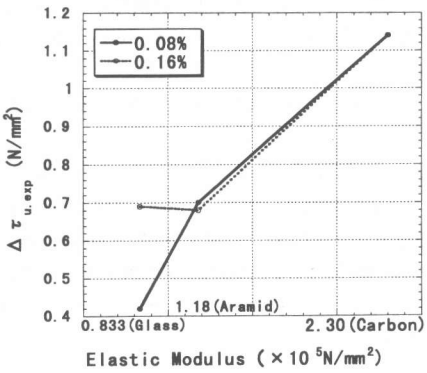

Figure 6: $\Delta\tau_{u.exp}$ – elastic modulus relationship

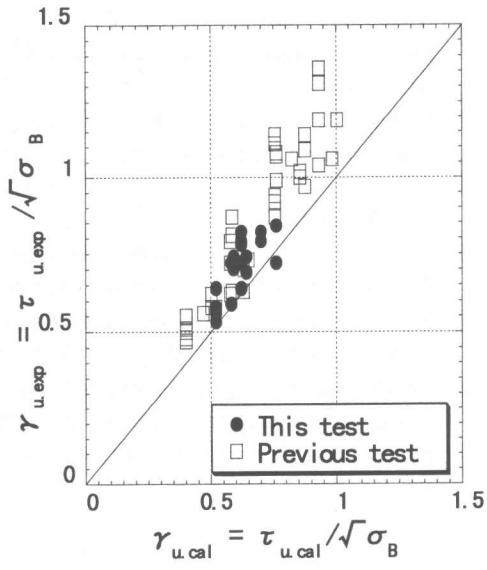

Figure 7: Non dimension bond strength experiment - calculated

3.5 TENSILE STRAIN LEVEL OF FRP SHEET

It is very important to know the maximum sheet strain throughout the entire loading. Figure 8 shows the relationship between the load and strain of FRP sheet. The sheet strain at the level of $\tau_{u.exp}$ and after that at the level of 0.9 $\tau_{u.exp}$ and 0.8 $\tau_{u.exp}$ in the falling branch. It is interesting that the strain decrease as the amount of sheet increase and the maximum strain occurs not at the peak load but after the peak load. The maximum strains of FRP sheet stay within about 33% at largest of its ultimate strain regardless of type of sheet.

4. CONCLUSION

The following remarks were obtained from twenty cantilever type specimens:(1) Bond strength increase and the slope of falling branch after peak load become more gentle as p_{wf} increase. (2) Bond stress carried by sheet confinement, $\Delta\tau_{u.exp}$ increase with proportional to the elastic modulus of used sheet. (3) The design equation predict the bond strength very well and rather in safety side.

ACKNOWLEDGEMENTS

The authors acknowledge the material supply provided by the Association of SR-CF Engineering and Showa Highpolymer CO., LTD., and thank graduate students at Toyohashi Institute of Technology including Ms. Yamazaki and Mr. Oda for providing assistant in experiments and data analyses.

REFERENCES

1. Architecture Institute of Japan(1998), "Application of fiber reinforced polymer to concrete structures," AIJ-9809-01000,pp88-91
2. Matsuno,K. et al., "Bond Splitting Strength of Reinforced Concrete Members Confined with FRP Sheet," Proceeding of the JCI, Vol.21,No3, pp.1483-1488,1999
3. Yamazaki,K. et al., "Bond Splitting Strength of Reinforced Concrete Members Confined with FRP Sheet," Summaries of Technical Papers of Annual Meeting AIJ, Structures IV,pp.353-354, 2000
4. Fujii,S. and Morita,S., "Splitting Bond Capacities of Deformed Bars, Part 2, "Proposed Ultimate Strength Equation for Splitting Bond Failure,"Transactions of AIJ, Vol.319, pp.47-55,Nov.1982

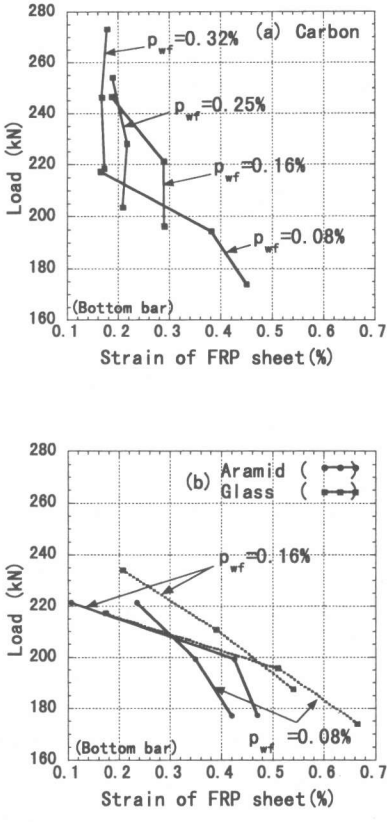

Figure 8: Load – strain of FRP sheet relationship